Investigating the Cell-Uptake of Guanidinium-Rich RAFT Polymers: Impact of Comonomer and Monomer Distribution

Liam Martin,[†,⊥] Raoul Peltier,[†,⊥] Agnès Kuroki,[†] James Town,[†] and Sébastien Perrier [†,‡,§]

[†] Department of Chemistry, University of Warwick, CV4 7AL, United Kingdom.

[‡] Warwick Medical School, University of Warwick, Coventry CV4 7AL, United Kingdom.

[§]Faculty of Pharmacy and Pharmaceutical Sciences, Monash University, VIC 3052, Australia.

Keywords: Cell Uptake, Drug delivery, Cell-penetrating, Arginine, Copolymer, RAFT polymerisation.

A range of well-defined guanidinium-rich linear polymers with demonstrable efficiency for cellular internalisation were developed. A protected guanidinium-functional acrylamide monomer (di-Boc-guanidinium ethyl acrylamide, GEA^{diBoc}) was synthesised and then polymerised *via* RAFT polymerisation to yield well-defined homopolymers, which were then deprotected and functionalised with a fluorescein dye to observe and quantify their cellular uptake. The cellular uptake of these homopolymers was first compared to polyArginine analogues, which are commonly used in modern drug delivery. Following this, a range of well-defined guanidinium-

rich copolymers were prepared in which the monomer distribution was varied using a convenient one-pot sequential RAFT polymerisation approach. Systematic quantification of the cell uptake of these compounds, supported by fluorescent confocal microscopy data, revealed that while the overall hydrophobicity of the resulting copolymers has a direct impact on the amount of copolymer taken up by cells, the distribution of monomers has an influence on both the extent of uptake and the relative extent to which each route of internalisation (endocytosis *vs* direct translocation) is exploited.

1. INTRODUCTION

The use of polymers as vectors for enhanced drug delivery is now well recognised and continues to receive enormous interest within the scientific community. Amongst the many advantages that polymeric systems can offer in pharmaceutical applications, the ability to facilitate the intracellular trafficking of molecular cargo is one of the most desirable.[1] Various aspects of polymeric architecture have been demonstrated to influence polymer uptake by cells, including primary microstructure (chain length, tacticity etc.), topology (linear, branched, brush and star polymers) and self-assembly behavior (vesicles, micelles and worm-like micelles).[2, 3] Linear copolymers are particularly appealing for drug delivery applications since they are synthetically easy to access, yet benefit from the properties of two or more chemically-distinct monomers in a single polymer chain, while the overall composition (amount of each monomer type), distribution of monomers and overall polymer length can be readily varied using controlled polymerisation techniques. Until recently, these systems were for the most part restricted to either statistically distributed copolymers, or self-assembled amphiphilic diblock copolymers, while the fundamental influence

of monomer distribution has remained somewhat under-explored. In recent years, reversible deactivation radical polymerisation (RDRP) methods such as reversible addition-fragmentation chain transfer (RAFT) polymerisation and Cu(0)-mediated radical polymerisation have granted ready access to intermediate levels of monomer distribution in the form of multiblock copolymers.[4-12] With this comes an opportunity to understand the influence of monomer distribution on biological function on a more fundamental level. We recently studied the effect of monomer distribution on the uptake of fully hydrophilic copolymers composed of a trio of biologically-passive acrylamide monomers, dimethylacrylamide (DMA), 4-acryloylmorpholine (NAM) and *N*-hydroxyethyl acrylamide (HEA), demonstrating that monomer distribution had little to no intrinsic impact on cellular uptake when the polymer chains are biologically-inert.[13] However, dramatically different conclusions could be expected when at least one monomer with biological activity is introduced into such systems.

Arginine-rich cell-penetrating peptides such as the Tat peptide and polyArginines have generated a lot interest in the field of drug delivery due to their proficiency for permeating cellular membranes. These low molar mass cationic peptides were shown to cross the cell membrane of mammalian cells mostly *via* an endocytotic-independent pathway,[14] however it should be noted that they also undergo endocytosis to some extent.[15] This behavior is largely attributed to their guanidinium-rich primary structures rather than the formation of higher-order (i.e. secondary or tertiary) structure.[16] The direct mechanism of cell-entry, while still debated, is thought to proceed *via* interaction of the positively charged guanidinium groups with negatively charged lipid membranes, thus disturbing the membrane structure.[17] Various theories, in particular based on the role of counter-ions, have been suggested as a possible explanation for the enhanced uptake of Arginine-rich macromolecules compared to those containing other positively charged amino acids

such as Lysines.[18, 19] Nonetheless, the use of the so-called "Arginine-magic" is highly appealing and as such is frequently exploited to facilitate the intracellular delivery of (macro)molecular cargo. However, the use of peptides is restrictive in scope in terms of accessible architecture, limited to low molar mass linear peptides, and moreover solid-phase synthesis can be a time-consuming and expensive process. As a result, polymeric systems similarly rich in guanidinium-moieties have been explored and represent a promising alternative to peptides for enhanced cellular internalisation. Wender and co-workers have applied this design concept to an extensive variety of polymeric backbones including poly-peptoids,[20] carbamates,[21] carbonates,[22] and phosphoesters,[23] with demonstrable efficiency for cellular uptake. RDRP techniques have also been used to prepare well-defined copolymers containing guanidinium pendant groups. McCormick and co-workers have studied fully hydrophilic guanidinium-rich methacrylamide copolymers for antimicrobial activity, cell-penetration and cell transfection.[24-26] In another example, Koschek and co-workers used RAFT polymerisation to prepare a small library of Arginine-containing polymer conjugates and studied the effect of charge and charge distribution on cellular uptake.[27]

Among the various factors which can affect the cellular uptake of polymers, hydrophobicity has been found to play a particularly important role. Increasing the overall hydrophobicity of polymeric systems is an effective approach towards promoting interaction between the cationic polymer chains and cellular membranes.[28] The nature of the polymer backbone can strongly influence the overall hydrophobicity of the polymer chains, and thus their cellular interaction. For example, Tew and co-workers investigated the delivery of siRNA or proteins using guanidinium-rich polymers with different backbone composition (methacrylate, styrenic and noroborene), and observed that polymers possessing increased hydrophobicity resulted in enhanced intracellular

delivery, although it was stressed that the type and amount hydrophobicity is a crucial factor.[29] An altogether simpler approach towards tuning hydrophobicity entails incorporating both cationic and hydrophobic monomers through copolymerisation to generate amphiphilic polymer chains. Indeed, several studies have shown that increasing the overall hydrophobicity of cationic polymers through copolymerisation may lead to enhanced cellular uptake.[29-35] However, despite the widespread use of these systems, the fundamental influence of monomer distribution on the cellular uptake of cationic copolymer systems has received little attention, since previous studies focus on amphiphilic copolymers that tend to self-assemble or fold in aqueous solution.[34, 36] This is especially true for fully-soluble guanidinium-rich polymers, for which the effect of monomer distribution on cellular internalisation remains unexplored.

In this work, we investigate the influence of monomer distribution on the cellular uptake of fully soluble copolymers containing a mixture of guanidinium-functional monomer and less hydrophilic neutral monomers. Well-defined guanidinium-rich homopolymers and copolymers were prepared *via* RAFT polymerisation. Firstly, low molar mass poly(guanidine ethyl acrylamide) (pGEA) homopolymers with narrow molar mass distribution ($Đ$) were compared to monodisperse polyArginine analogues possessing an equivalent number of arginine residues to determine the extent and the mechanism by which the polymers enter cells. Following this, we prepared a range of low molar mass (less than 6000 $g.mol^{-1}$) copolymers each containing a 50 % molar ratio of guanidinium-functional GEA monomer with one of two biologically passive (and less hydrophilic) comonomers, varying the block structure (statistical, tetrablock and diblock) to investigate the impact of co-monomer type and monomer distribution on their cellular uptake.

2. MATERIALS AND METHODS

2.1 Materials. 5-FITC cadaverine was obtained from AAT Bioquest and used as received. 5-((5-aminopentyl)thioureidyl)fluorescein, trifluoroacetate salt (fluorescein cadaverine) was obtained from Biotium and used as received. Trifluoroacetic acid (TFA, 99 %) was obtained from Acros Organics and used as received. 1,1,1,3,3,3-Hexafluoro-2-propanol (HFIP), 4-methylmorpholine (NMM) (99 %) and Triisopropylsilane (TIPS) (98 %) were obtained from Alfa Aesar and used as received. 1,3-Bis(*tert*-butoxycarbonyl)-2-methyl-2-thiopseudourea (98 %), ethylenediamine, was obtained from Aldrich and *N*-Ethyldiisopropylamine (DIPEA) was obtained from Fluka and used as received. O-(1*H*-6-Chlorobenzotriazole-1-yl)-1,1,3,3-tetramethyluronium hexafluorophosphate (HCTU), 2-Chlorotrityl chloride resin and Fmoc-protected amino acids were purchased from Iris Biotech. And used as received. *N,N*-dimethylacrylamide (DMA, 99 %) and *N*-hydroxyethyl acrylamide (HEA, 97 %) were obtained from Sigma Aldrich and passed through basic alumina to remove inhibitor. DMF, ethyl acetate, hexane, methanol, ethanol, acryloyl chloride, 1,4-dioxane was obtained from Fisher Scientific and used as received. 2,2′-Azobis[2-(2-imidazolin-2-yl)propane] dihydrochloride (VA-044) was obtained from Wako and used as received. The chain transfer agent 2-(((butylthio)-carbonothioyl)thio)propanoic acid (called (propanoic acid)yl butyl trithiocarbonate, PABTC in this work),was prepared according to a previously reported procedure.[37]

2.2. Synthesis and characterisation of compounds. Synthesis of polyArginine and fluorescein-polyArginine, synthesis of 1,3-Di-Boc-guanidinoethyl acrylamide (GEA^{diBoc}) monomer, monomer characterisation *via* NMR and Mass Spectrometry, homopolymerisation, block copolymerisation, deprotection of polymers and attachment of fluorescein cadaverine are described in Supporting Information.

2.3. Size exclusion chromatography (SEC). SEC was conducted using an Agilent 390-LC MDS instrument equipped with differential refractive index (DRI), viscometry (VS), dual angle light scattering (LS) and dual wavelength UV detectors. The liquid chromatography system used 2 x PLgel Mixed D columns (300 x 7.5 mm) and a PLgel 5 μm guard column. The dimethlyformamide (DMF) eluent contained 5 mmol NH_4BF_4 as additive. Samples were run at 1 $ml.min^{-1}$ at 50 °C. Analyte samples were filtered through a polytetrafluoroethylene (PTFE) membrane with 0.2 μm pore size prior to injection. Poly(methyl methacrylate) (PMMA) narrow standards (Agilent EasyVials) were used to calibrate the SEC system. Experimental $M_{n,SEC}$ and $Đ$ (M_w / M_n) of synthesised polymers were determined using Agilent GPC software.

2.4. Nuclear magnetic resonance spectroscopy (NMR). ^{1}H NMR spectra were recorded on a Bruker Avance III HD 300 MHz, Bruker Avance III HD 400 MHz or Bruker Avance III HD 500 MHz spectrometer at 298 K. The theoretical number-average molar mass ($M_{n,th}$) of the RAFT polymers was calculated using the following equation:

$$M_{n,th} = \frac{[M]_0 p M_M}{[CTA]_0} + M_{CTA}$$

Where $[M]_0$ and $[CTA]_0$ are the initial concentrations (in $mol.L^{-1}$) of monomer and chain transfer agent respectively; p is the monomer conversion (as determined by ^{1}H NMR); M_M and M_{CTA} are the molar masses ($g.mol^{-1}$) of the monomer and CTA respectively.

2.5. Analytical high performance liquid chromatography (HPLC). HPLC analysis was done on an Agilent 1260 Infinity series stack equipped with an Agilent 1260 variable wavelength detector and an Agilent 1260 fluorescence detector. The HPLC was fitted with a Phenomenex Luna® C18 (250 × 4.6 mm) column with 5 μm micron packing (100 Å). Mobile phase A consisted of water containing 0.05 % TFA, mobile Phase B consisted of acetonitrile containing 0.05 % TFA. The gradient used for HPLC analysis increased from 5 % to 95 % B over 40 minutes. Detection

was achieved *via* monitoring at 309 nm for the polymers (trithiocarbonate group) and 220 nm for the peptides (amide bond). Fluorescent detection was monitored using λ_{ex} = 490 nm and λ_{em} = 525 nm.

2.6. Dynamic light scattering (DLS). Size measurements were conducted on a Malvern Zetasizer Nano-ZS at 25 °C with a 4 mW He-Ne 633 nm laser at a scattering angle of 173 ° (back scattering), assuming the refractive of PMMA. The measurements were repeated three times with automatic attenuation selection and measurement position. Results were analyzed using Malvern DTS 6.20 software.

2.7 Maldi-TOF. Samples for Maldi-TOF measurements were mixed at 1 $mg.mL^{-1}$ into 50:50 deionised water/THF with 0.1 $mg.ml^{-1}$ NaI and 0.1 $mol.L^{-1}$ chloroacetic acid, 15 $mg.mL^{-1}$ of Super Dihydroxybenzoic acid (SDHB). 0.5 µL of the solution was then deposited onto an MTP384 ground steel target plate and analyzed using a Bruker UltrafleXtreme Maldi TOF/TOF analyzer. The samples were analyzed in a reflectron positive mode with a 21 kV reflecting voltage and an 18 kV detection voltage, using a 355 nm laser set to 26 % laser power.

2.8. Cell lines and cell culture. MDA-MB-231 cells were cultivated in Dulbecco's modified eagle medium (DMEM) supplemented with 10 % fetal bovine serum and 2 mM L-glutamine. Caco2 cells were cultivated in 1:1 DMEM:F12 medium supplemented with 10 % fetal bovine serum and 2 mM L-glutamine.

2.9. Cytotoxicity assays. Cell viability was tested using a standard protocol for the XTT assay.[38] Briefly, Caco2 cells were seeded in 96 well plates at a density of 1×10^4 cells per well and allowed to attach for 24 h. The culture medium was replaced with fresh medium containing a series of dilutions of polymers or peptides (100, 50, 10, 1 and 0.1 $\mu mol.L^{-1}$). Following 24 h incubation, the medium was replaced with fresh medium and 25 uL of a solution of XTT (1 $mg.mL^{-1}$) containing

N-methyl dibenzopyrazine methyl sulfate (PMS) (25 μmol.L^{-1}) in medium was added. Cells were further incubated for 16 h. Absorbance of samples were then measured using a Synergy HTX plate reader at 450 nm and 650 nm (background).

2.10. Confocal microscopy. MDA-MB-231 cells were chosen for confocal imaging as they are easier to image than Caco2 which grow as aggregates. Briefly, MDA-MB-231 cells were seeded in an 8-well ibidi plate at a density of 1×10^4 cells per well and allowed to grow for 24 hours prior to the experiment. The culture medium was replaced with fresh media containing the compounds at either 5 μmol.L^{-1} (R_{20}, $pGEA_{20}$) or 2 μmol.L^{-1} (DMA_{stat}, $DMA_{diblock}$) previously prepared from stock solutions in pure water at 500 μmol.L^{-1}. For incubation at 4 °C, cells were cooled down 30 minutes prior to incubation with the compounds. Cells were then left to incubate for either 2 h or 16 h at the indicated temperature. Lysotracker Red^{TM} was added to the appropriate well 2 h prior to the end of incubation following supplier recommendations. Hoescht 33342 was added to all the wells 15 minutes prior to the end of the incubation to stain the nucleus of the cells. Following incubation, cells were washed with warm medium twice, and fresh medium was added. Confocal microscopy images were taken on a Leica TCS SP5 (Carl Zeiss, Germany) at a temperature of either 37 °C or at room temperature (for 4 °C experiments), using sequential scanning for each channel. Excitation/Emission used for measurement are used as follow: nucleus channel (405 / 410-458 nm), fluorescein channel (488 / 511-564 nm), Lysotracker Red^{TM} (561 / 589 - 708nm).

2.11. Cellular uptake experiments. Cellular uptake was quantified *via* measurement of the intracellular fluorescence following incubation with fluorescein-labelled polymers or peptide. Briefly, MDA-MB-231 cells or Caco2 cells were seeded into a black 96 well plate with a clear bottom, at a density of 5000 cells per well, and were allowed to grow for 24 h. The culture medium was replaced with fresh media containing the compounds at either 5 μmol.L^{-1} (R_9, R_{20}, $pGEA_9$,

pGEA$_{20}$, pGEA$_{40}$) or 2 μmol.L^{-1} (pGEA$_{40}$, pDMA$_{40}$, pHEAm$_{40}$, copolymers) previously prepared from stock solutions in pure water at 500 μmol.L^{-1}. For incubation at 4 °C, cells were cooled down 30 minutes prior to incubation with the compounds. Cells were then left to incubate for either 2 h or 16 h at the indicated temperature. Hoescht 33342 was added to all the wells 15 minutes prior to the end of the incubation to stain the nucleus of the cells. Following incubation, cells were washed with medium twice, and fresh medium was added. Each well was then imaged individually using a Cytation3 Cell Imaging Multi-Mode ReaderTM from Biotek®. Using Gen5™ software, single cells were isolated using the blue channel corresponding to Hoescht 33342. An area extending the nucleus area of the cells by 7 μM or 20 μM for MDA-MB-231 or Caco2 cells, respectively, was arbitrarily defined as the cell area. Following background reduction using a rolling ball model (30 μM), intracellular fluorescence in individual cells was quantified using the fluorescence associated with fluorescein (GFP filter, λ_{ex} = 469 nm, λ_{em} = 525 nm) in the area of each cell. The average mean of fluorescence in each well was then used as the sample value. The data given are representative of two separate experiments where each sample was measured in triplicate (n = 4). All errors reported correspond to the standard deviation from the mean.

3. RESULTS AND DISCUSSION

3.1. Monomer Synthesis. The polymers synthesised in this work were all comprised of acrylamide monomers. Due to their high k_p and $k_p/(k_t)^{1/2}$, acrylamide monomers may typically be polymerised to quantitative monomer conversion using only very low initiator concentrations, thereby preserving a high fraction of living ω-chain ends. With such a system, multiple chain-extensions may be conducted to generate (in one-pot) well-defined (multi)block copolymers.[5-7, 9] Acrylamides are also advantageous in that they are generally not prone to side reactions of transfer

during polymerisation and are stable towards hydrolysis. Hence, we designed an acrylamide monomer bearing a pendant (Boc-protected) guanidine moiety, whose resulting polymers, once deprotected, would yield polymeric chains with pendant guanidinium moieties similar to polyArginine. The di-Boc-protected guanidine ethyl acrylamide (GEA^{diBoc}) was prepared in a two-step synthesis as shown in **Scheme 1**. Since the beginning of this work, this monomer synthesis has been reported, albeit as an intermediate which was not purified or characterised.[39]

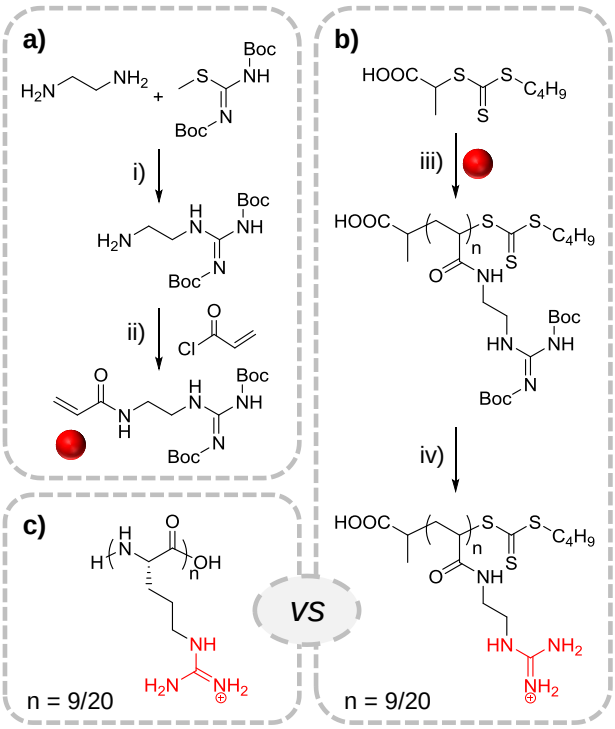

Scheme 1. Synthesis of GEA^{diBoc} **(a)**; i) DCM, 3 h. ii) TEA, DCM, < 10 °C, 16 h. Synthesis of $pGEA^{diBoc}$ *via* RAFT polymerisation **(b)**; iii) VA-044, 1,4-dioxane/H_2O, 45 °C, 7 h. iv) Deprotection of $pGEA^{diBoc}$; iv) TFA/TIPS/H_2O, RT, 3 h. Structure of polyArginine **(c)**.

3.2. Synthesis of guanidinium-rich homopolymers *via* RAFT polymerisation. Having designed and synthesised the protected guanidinium-functional acrylamide monomer, we initially

wanted to compare the proficiency of well-defined low molar mass poly(guanidine ethyl acrylamide) (pGEA) homopolymers for cellular internalisation with the commonly-used monodisperse polyArginine analogues prepared *via* solid phase peptide synthesis (SPPS). The principal difference between these classes of guanidinium-rich compounds are their polymeric backbones, with the vinyl backbone of the RAFT polymers expected to be more hydrophobic than their peptidic equivalents (**Scheme 1)**. SPPS by nature enables near-perfect control over monomer sequence and the length of peptide chains (up to a certain number of residues), which is beyond the scope of RDRP. However, considering this part of the study concerns homopolymers, polymers with equivalent DP_n and narrow molar mass distributions ($Đ$), as may be obtained using RDRP, are still expected to provide a valid comparison. The GEA monomer was polymerised in its protected form (GEA^{diBoc}) using (propanoic acid)yl butyl trithiocarbonate (PABTC) as chain transfer agent (CTA). This CTA was selected since it affords control over the polymerisation of acrylamide monomers, while the COOH of the R-group may be readily exploited to functionalise the α-chain end of the resulting polymers. RAFT polymerisations were conducted at 45 °C using 1,4-dioxane/water as a solvent system and 2,2′-Azobis[2-(2-imidazolin-2-yl)propane] dihydrochloride (VA-044) as the initiator. Well-defined $pGEA^{diBoc}$ homopolymers were prepared with a DP_n of 9 ($pGEA_9$) or 20 ($pGEA_{20}$) as determined by ^{1}H NMR (shown for $pGEA_9$ in **Fig. S2**), with DMF-SEC revealing monomodal populations with narrow molar mass distributions ($Đ$ = 1.1) (**Table 1** and **Fig. S2**). Further details on polymerisation conditions and synthesis of the two peptide controls (R_9 and R_{20}) are provided in the Supporting Information.

Table 1. Summary of homo- and copolymers prepared *via* RAFT polymerisation.

Compound	Composition	$M_{n,th}$[a] (g.mol^{-1})	$M_{n,expt}$[b] (g.mol^{-1})	$Đ_{expt}$[b]
$pGEA_9$	$pGEA_9$	1650[c] (3450)	3100	1.12
$pGEA_{20}$	$pGEA_{20}$	3400[c] (7350)	5600	1.10
$pGEA_{40}$	$pGEA_{40}$	6600[c] (14500)	9750	1.14
DMA_{stat}	$pDMA_{20}$-*st*-$pGEA_{20}$		8600	1.10
DMA_{tetra}	$pDMA_{10}$-*b*-$pGEA_{10}$-*b*-$pDMA_{10}$-*b*-$pGEA_{10}$	5400[c] (9350)	9400	1.08
$DMA_{diblock}$	$pDMA_{20}$-*b*-$pGEA_{20}$		8050	1.11
HEA_{stat}	$pHEA_{20}$-*st*-$pGEA_{20}$		9200	1.12
HEA_{tetra}	$pHEA_{10}$-*b*-$pGEA_{10}$-*b*-$pHEA_{10}$-*b*-$pGEA_{10}$	5700[c] (9650)	9950	1.17
$HEA_{diblock}$	$pHEA_{20}$-*b*-$pGEA_{20}$		9700	1.13

[a] Determined using equation 1 (experimental part).

[b] Determined using DMF-SEC with PMMA narrow standards, polymers are in their Boc-protected form.

[c] Theoretical molar mass of polymers following deprotection.

The experimental molar masses ($M_{n,expt}$) obtained for both $pGEA_9$ and $pGEA_{20}$, in their protected form, are slightly below the theoretically calculated values (**Table 1**), which may be attributed to a difference in hydrodynamic volume between $pGEA^{diBoc}$ and the PMMA narrow standards used to calibrate the SEC system. Deprotection of the $pGEA^{diBoc}$ homopolymers to yield well-defined pGEA with cationic guanidinium pendant groups was achieved using trifluoroacetic acid (TFA) in the presence of scavengers. Successful removal of the Boc protecting groups to yield the desired guanidinium-pendant groups was confirmed using ^{1}H NMR, as exemplified using $pGEA_9$ in **Fig. S2**.

For cell uptake studies, the compounds were functionalised with a fluorescein derivative. Peptides R_9 and R_{20} were modified with fluorescein-NHS at their *N*-terminus directly on the resin and the excess dye washed off before proceeding to the cleavage step. Fluorescein cadaverine was introduced to the α-chain end of $pGEA_9$ and $pGEA_{20}$ *via* HCTU coupling in DMF. Removal of excess free dye was achieved *via* extensive dialysis and was quantified using HPLC until less than 10 % of free dye remained. Fluorescent HPLC traces of the final compounds are presented in **Fig. S3**. In the case of $pGEA_9$ and $pGEA_{20}$ two peaks were observed, however HPLC conducted prior to dye attachment revealed only a single peak (**Fig. S4**). Matrix assisted laser desorption/ionisation-time of flight mass spectrometry (Maldi-TOF-MS) analysis of $pGEA_9$ (**Fig. S5**) suggests the presence of two side reactions, namely removal of the trithiocarbonate end of the polymer and partial hydrolysis of the thioamide bond of fluorescein cadaverine. These side reactions may occur either during the measurement as part of the fractionation process, or during the dialysis step, which may account for the two peaks observed in HPLC. To account for any differences in the fluorescence intensity for each compound, a fluorescence correction factor was calculated from the slope of their respective fluorescence profiles **(Table S4)**.[13] To ensure that the presence of hydrolysed dye does not affect uptake studies, control samples in which fluorescein cadaverine was incubated in the presence of cells for 16 h were carried out, which revealed no intracellular fluorescence at the concentrations used elsewhere in this study **(Table S4)**.

3.3. Comparison of pGEA homopolymers and polyArginines. Acute toxicity of the polyArginines (R_9 and R_{20}) and guanidinium-rich pGEA RAFT homopolymers ($pGEA_9$ and $pGEA_{20}$) was assessed using colorectal adenocarcinoma Caco2 cells. Peptides R_9 and R_{20} were found to be non-toxic at concentrations up to 100 μM following 24 h incubation **(Fig. S6)**, which

is consistent with previous observations in the literature.[40] In contrast, incubation with the analogous RAFT polymers $pGEA_9$ and $pGEA_{20}$ resulted in decreased cell viability at concentrations above 50 μM and 10 μM, respectively. To assess whether the comparably higher toxicity of the RAFT polymers could be due to enhanced uptake of the compounds, we proceeded to study their intracellular uptake. With delivery of anticancer drugs in focus, this was conducted on both colorectal adenocarcinoma Caco2 cells and human breast adenocarcinoma MDA-MB-231 cells, two well-established model cancer cell lines.

MDA-MB-231 and Caco2 cells were incubated with non-toxic concentrations of the fluorescent compounds (5 μM) for 2 or 16 h, and uptake was quantified by measuring the intracellular fluorescence **(Fig. 1 and S7)**. Levels of intracellular uptake measured in MDA for pGEA RAFT polymers were found to be higher in comparison to their polyArginines analogues of similar length (at both 2 and 16 h of incubation). This observation may be attributed to greater hydrophobicity of the vinyl backbone of pGEA relative to the amide backbone of polyArginines, as demonstrated by the later retention times observed in HPLC for the polymers **(Fig. S3)**. This explanation is in accordance with a recent study on the delivery of green fluorescent protein by guanidinium-based polymers with various backbone chemistry, which found that an increase in the overall hydrophobicity of cell-penetrating systems typically lead to enhanced cellular uptake.[29] At equimolar concentrations, the higher molar mass compounds (R_{20} and $pGEA_{20}$) are internalised more than their respective lower molar mass equivalents, likely due to the increased number of guanidinium residues in solution. Mitchell and co-workers demonstrated than the uptake of polyArginine peptides by Jurkat cells after 5 min of incubation increased as a function of peptide length up to 15 residues, after which it starts to decrease.[41] The same study showed a linear increase in intracellular uptake as a function of time for a polyArginine (R_7), which was also observed for

pGEA$_9$ and pGEA$_{20}$ in the present study. In contrast, the intracellular uptake of R_9 or R_{20} was found to be relatively time-independent, except in MDA cells where the intracellular fluorescence following 2 h incubation with R_9 was found to be reproducibly greater than after 16 h. Futaki and co-workers reported a loss of intracellular fluorescence associated with the Arginine-rich CPP HIV-1 Rev(34-50) over time, which they attributed to intracellular degradation of the peptide rather than leakage from the cells.[42] The fact that this is only observed for the low molar mass polyArginine (R_9) in our case may indicate that the mechanism of cellular uptake for this compound may differ from the other compounds studied.

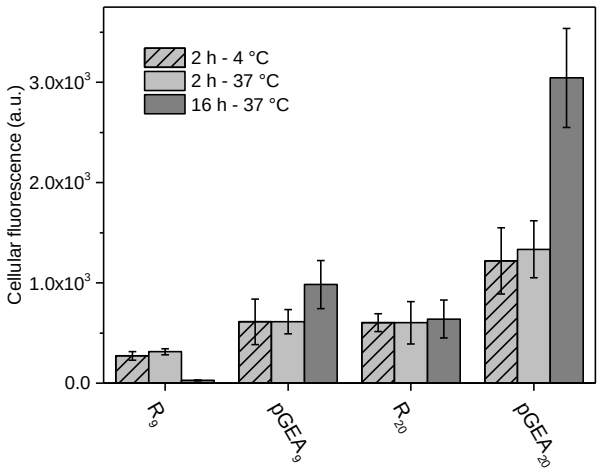

Figure 1. Comparison of the cell uptake of polyArginine peptides *vs* RAFT polymer equivalents. Fluorescence intensity measured in MDA-MB-231 cells incubated with 5 μM of R_9, pGEA$_9$, R_{20} and pGEA$_{20}$ for the indicated time and temperature.

To further explore the mechanism of uptake, the ability of the compounds to enter cells *via* non-endocytotic pathways (i.e. passive membrane translocation) was quantified by incubating the samples at 4 °C (**Fig. 1** and **S7** for MDA-MB-231 and Caco2 cells, respectively). As expected, the

extent of cellular uptake in MDA-231-MB cells at 4 °C was relatively similar to that observed at 37 °C (after 2 h incubation) for all four compounds, which is consistent with other reports that guanidinium-rich macromolecules are mostly internalised *via* passive crossing.[43] Similar results were observed in Caco2, with the exception of $pGEA_{20}$ which is not conclusive. The intracellular uptake of R_{20} and $pGEA_{20}$ by MDA-MB-231 cells was further studied using confocal microscopy (**Fig. 2**). Incubation with either compound at 37 °C, for 2 h or 16 h, revealed patterns of punctate fluorescent within the cells, characteristic of vesicular uptake. Furthermore, co-localisation of these puncta with Lysotracker™ Red indicate that the majority of the internalised R_{20} and $pGEA_{20}$ were located in lysosomal compartments of cells after 2 h or more. When incubation was conducted at 4 °C (2 h), an altogether different distribution of intracellular fluorescence was observed, with fluorescence instead found diffused throughout the cell (**Fig. 2**). In the case of R_{20}, cells were observed to be entirely fluorescent, including the nucleus. Similar observations were made by Fretz and co-workers in a thorough study of the influence of temperature on the cell uptake of L-octaarginine.[43] With $pGEA_{20}$ the dispersion of fluorescence across each cell is less profound, and indeed does not cross into the nucleus area of the cells, possibly due to a weaker membrane permeation potential (**Fig. 2**).

Taken together, these results suggest a relatively similar mechanism of uptake for both $pGEA_{20}$ and R_{20} with passive permeation through the cell membranes being the main uptake pathway. Yet, a smaller amount of compound is taken up *via* endocytosis at 37 °C, resulting in concentrated pockets of fluorescent compound in the endosomes and lysosomes, arising in the bright puncta observed in the microscopy images.

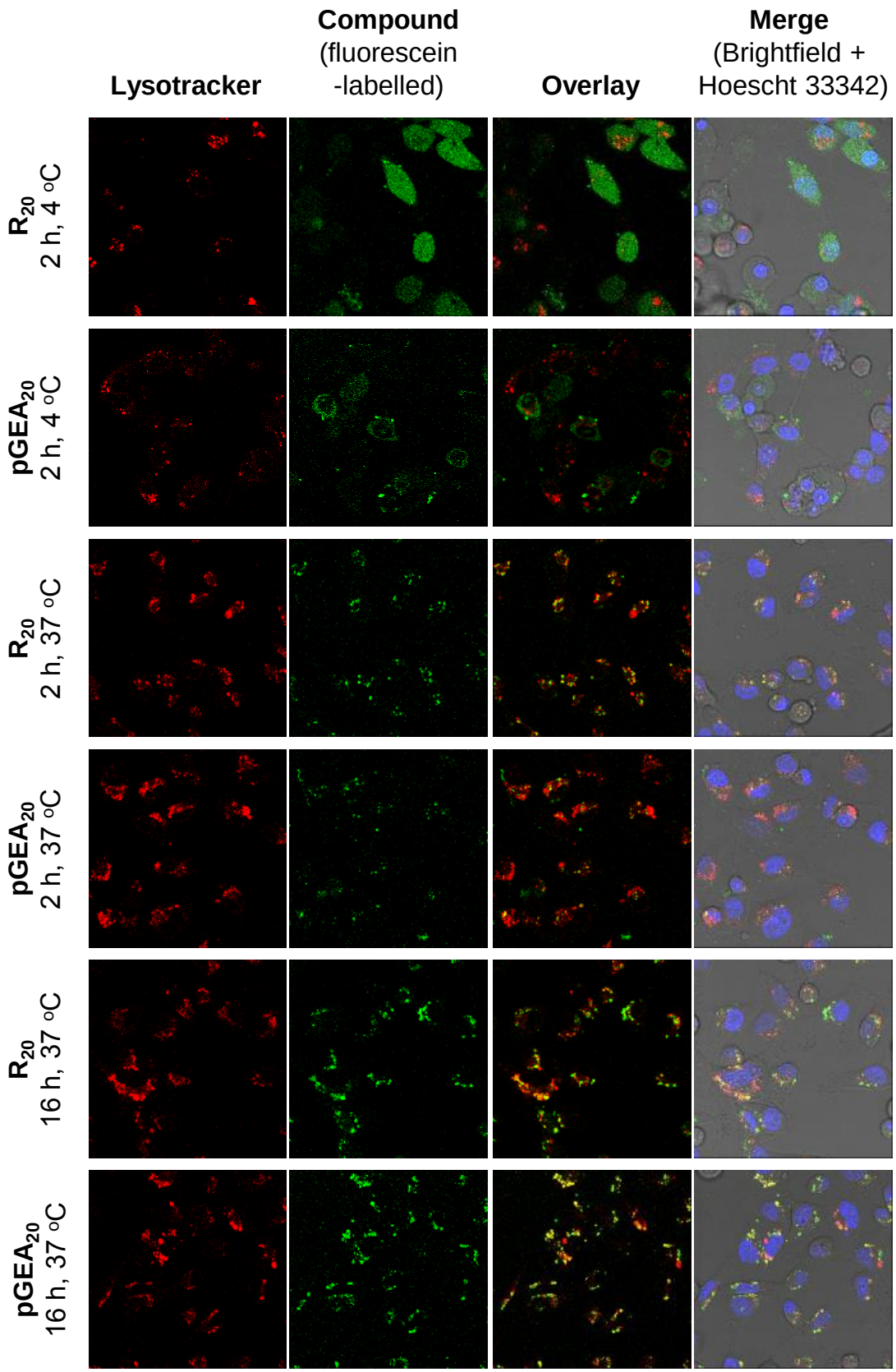
Lysotracker
Compound (fluorescein -labelled)
Overlay
Merge (Brightfield + Hoescht 33342)
R20 2 h, 4 °C
pGEA20 2 h, 4 °C
R20 2 h, 37 °C
pGEA20 2 h, 37 °C
R20 16 h, 37 °C
pGEA20 16 h, 37 °C

1

Figure 2. Confocal microscopic images of the intracellular location of R_{20} and $pGEA_{20}$ in live MDA-MB-231 cells following incubation at the indicated time and temperature Cells were stained with Lysotracker™ Red and Hoechst 33342 to stain the lysosomes and nucleus, respectively. Co-localisation of the compounds with the lysosomes resulted in yellow spots in the overlay images.

3.4. Synthesis of guanidine-rich copolymers *via* RAFT polymerisation. Having established the propensity of the acrylamide-based pGEA RAFT polymers for cellular uptake, we proceeded to introduce hydrophobic comonomers into the system, investigating both the influence of comonomer and their distribution along the polymer backbone on cellular uptake. Two acrylamide monomers, *N*,*N*-dimethylacrylamide (DMA) and *N*-hydroxyethyl acrylamide (HEA) were selected for this study. These monomers are uncharged and, to the best of our knowledge, biologically inert. Their corresponding polymers are both more hydrophobic than pGEA, as indicated by HPLC traces of their respective homopolymers (**Fig. S15**), yet sufficiently hydrophilic to ensure the resulting copolymers do not self-assemble or aggregate in solution, allowing this study to investigate the fundamental influence of polymer microstructure on intracellular uptake.

A series of relatively low molar mass (< 6000 $g.mol^{-1}$) copolymers with an overall composition of 20 units of "active" GEA monomer and 20 units of "inactive" comonomer (DMA or HEA) were targeted, comprised of either one, two or four distinct blocks (statistical, diblock and tetrablock copolymer, respectively). These copolymers were prepared *via* RAFT polymerisation using conditions similar to those described above. A breakdown of all polymer synthesis is provided in the Supporting Information (**Table S1** and **S2**). Statistical copolymers DMA_{stat} and HEA_{stat} were prepared in a single polymerisation step conducted in dioxane/H_2O (80/20 *v/v*) at 45 °C. Near-quantitative monomer conversion was achieved within 5 h in each case and DMF-SEC indicated

the successful preparation of well-defined copolymer, exhibiting a monomodal population with only a small amount of low molar mass tailing (**Fig. 3**, **S8** and **S9**). The compositional drift of these statistical copolymers was assessed by following the polymerisation kinetics, where it was determined that each monomer is incorporated at a similar rate, indicating an equal distribution of each monomer along the polymer backbone (**Fig. S10** and **S11**). Meanwhile the diblock copolymers ($DMA_{diblock}$ and $HEA_{diblock}$) and tetrablock copolymers (DMA_{tetra} and HEA_{tetra}) were prepared *via* a one-pot sequential polymerisation approach (**Scheme 2**). In each case, the "inactive" monomer (DMA or HEA) was polymerised as the initial block under highly optimised conditions (high monomer concentration, water content and temperature) to achieve quantitative monomer conversion after only 2 h, with a high $[PABTC]_0/[VA\text{-}044]_0$ ratio (60 or more) and consequently a (theoretical) high fraction of living chains. For the synthesis of the subsequent block(s), in order to successfully incorporate the GEA^{diBoc} monomer, polymerisations were conducted at 45 °C (20 h per block) with substantially decreased monomer concentrations and an increased dioxane content (≈ 80 % of solvent composition). Nevertheless, relatively high $[PABTC]_0/[VA\text{-}044]_0$ ratios (the lowest for any block synthesis was ≈ 20) could be employed in all cases (**Table S2**). Near-quantitative monomer conversions (> 95 %) were achieved in all cases while DMF-SEC revealed a clear shift towards higher molar mass with each successive chain extension (**Fig. S8** and **S9**), with the final purified polymers possessing narrow molar mass distributions ($Đ$ < 1.2) (**Table 1** and **S3**).

The molar masses determined from DMF-SEC for each copolymer microstructure (statistical, tetrablock and diblock) were in relatively close agreement and indeed the chromatograms are found to overlap well (**Fig. S8 and S9**). The polymers were deprotected using TFA as with the pGEA homopolymers, with ^{1}H NMR confirming removal of the Boc protecting groups (shown for

both DMA_{stat} and HEA_{stat} in **Fig. S12** and **S13**). Dynamic light scattering (DLS) measurements conducted on the copolymer compounds confirm the absence of self-assembly behavior at a concentration of 100 mM in PBS, which is far higher than those used in this study (**Fig. S19**).

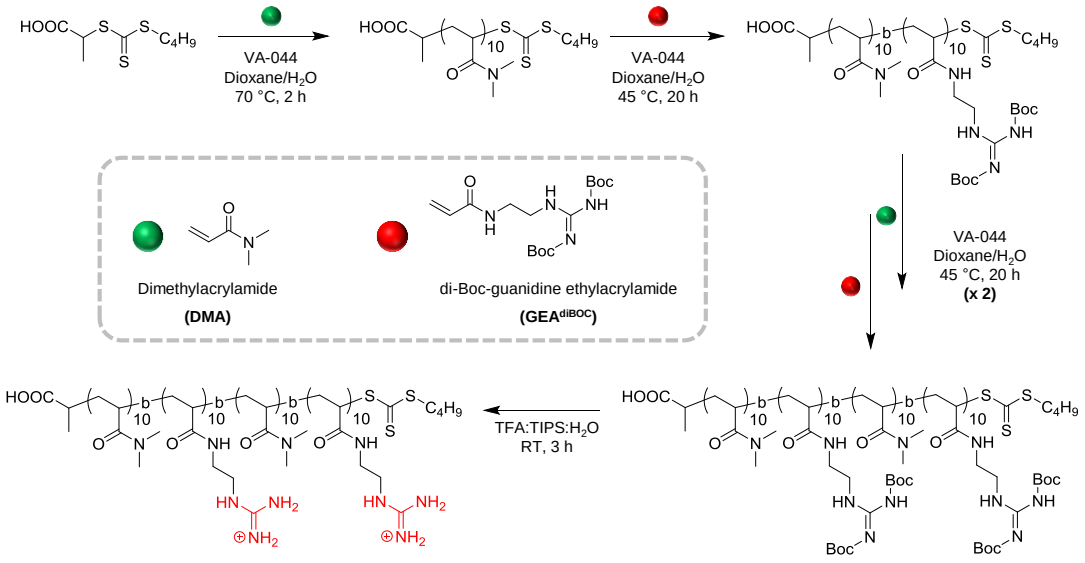

Scheme 2. Synthesis of $pDMA_{10}$-*b*-$pGEA_{10}$-*b*-$pDMA_{10}$-*b*-$pGEA_{10}$ tetrablock copolymer prepared *via* one-pot sequential addition RAFT polymerisation.

3.5. Influence of comonomer on cell uptake. Acute toxicity profiles for these six guanidinium-rich copolymers, as well as homopolymers of each monomer ($pGEA_{40}$, $pHEA_{40}$ and $pDMA_{40}$, **Table S3 and Fig. S14**) against Caco2 cells are shown in **Fig. S16**. Following the trend observed for $pGEA_9$ and $pGEA_{20}$, the higher molar mass $pGEA_{40}$ was found to be toxic at concentrations as low as 10 μM. In contrast, $pHEA_{40}$ and $pDMA_{40}$ did not appear to affect cell viability within the concentration range studied. The copolymers, each comprising on average 20 units of the cationic GEA monomer, exhibited toxicity comparable to that of $pGEA_{20}$. No clear trend was observed between toxicity and copolymer microstructure, with most compounds showing some toxicity at

concentrations above 10 μM, suggesting that copolymerisation of GEA with DMA and HEA does not inherently reduce toxicity.

Next, the polymers were labelled with a fluorescein cadaverine dye (Fluorescent HPLC shown in **Fig. S15**, corrected fluorescence shown in **Table S4**) and their uptake by MDA-MB-231 and Caco2 cell lines quantified (**Fig. 3**, **S17** and **S18**). As with $pGEA_9$ and $pGEA_{20}$, uptake of the copolymers was found to be dependent on incubation time at 37 °C, with cellular fluorescence generally increasing with longer incubation times (2 to 16 h). Interestingly, both DMA_{stat} and HEA_{stat} were taken up by cells more than $pGEA_{40}$, despite possessing half as many guanidinium moieties (on average) per polymer chain. We attribute this to an increase in the overall hydrophobicity of the polymers from the incorporation of the more hydrophobic comonomers. This is further supported by the observation that, in both of the cell lines studied, DMA_{stat} was internalised more than its less hydrophobic HEA-containing equivalent (HEA_{stat}), as indicated by the HPLC chromatograms of the final compounds (**Fig. S15**). This is consistent with reported literature that the overall hydrophobicity of (soluble) copolymer systems has an influence their cellular uptake behaviour.[28, 44] However, the more segmented copolymer microstructures (tetrablock and diblock copolymers) of DMA and HEA were not internalised more than $pGEA_{40}$, suggesting that the monomer distribution also has a strong influence on the extent, and possibly also the mechanism, of intracellular uptake.

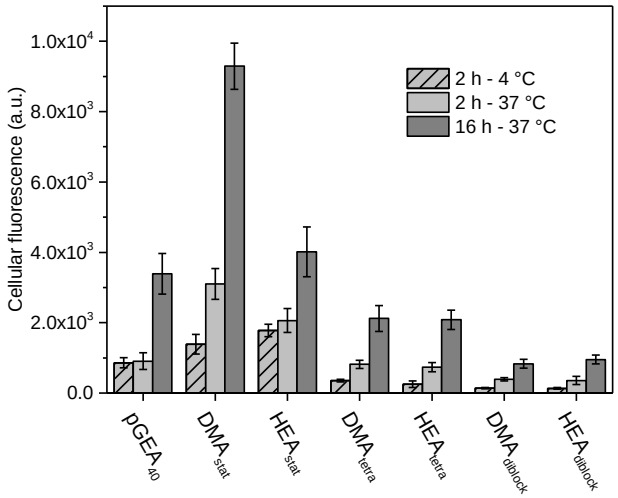

Figure 3. Comparison of the cell uptake of RAFT guanidinium-rich copolymers with various architecture (DP = 40). Fluorescence intensity measured in MDA-MB-231 cells incubated with 2 μM of DMA_{stat}, HEA_{stat}, DMA_{tetra}, HEA_{tetra}, $DMA_{diblock}$ and $HEA_{diblock}$ for the indicated time and temperature.

3.6. Influence of copolymer segmentation. Next, we proceeded to explore the impact of segregating the two distinct chemical functionalities. Results are reported in **Fig. 3** for MDA-MB-231 cells and **Fig. S17** for Caco2 cells. In both copolymer systems, increasing the segregation of comonomers from statistical to tetrablock to diblock copolymer resulted in a significant decrease in the extent of internalisation. With exception of DMA_{stat}, HPLC indicates that the hydrophilicity of the copolymers remain relatively similar regardless of microstructure, suggesting that differences in hydrophobicity cannot solely account for the differences in the extent of cell uptake observed (**Fig. S15**). Only considering hydrophobicity would fail to explain, for example, why HEA_{stat} is internalised more efficiently than $DMA_{diblock}$, since the latter is still expected to be more hydrophobic. Rather, the distribution of the cationic and hydrophobic moieties along the polymer backbone should be considered. Barz and co-workers reported that statistical copolymers

comprised of *N*-(2-hydroxypropyl)methacrylamide (HPMA) and lauryl methacrylate (LMA), which were shown to forms aggregates, entered cancer cells more efficiently than their micelle-forming block copolymer counterparts.[45] However, this should not be the case in our copolymer systems since they are fully hydrophilic, and indeed DLS does not indicate the occurrence of self-assembly for any compounds (**Fig. S19**). One possible explanation is the more even distribution of guanidinium groups in the statistical copolymers compared to the block copolymer equivalents. Condensing the guanidinium moieties into defined blocks on an already compact vinyl backbone could be expected to decrease the number of surface charge available, thus restricting electrostatic interaction with the negatively charged lipid membrane of cells, which may explain our observations. Rothbard and co-workers reported that the introduction of non-arginine spacer residues in polyArginine decamers could lead to improved uptake by Jurkat cells.[46] Indeed, they showed that decamers containing three non-arginine spacer residues were internalised more than a heptaArginine (R_7) itself.

In an attempt to understand this effect better, the cellular uptake was also measured at 4 °C. In contrast with the pGEA homopolymers, the copolymers generally experienced reduced internalisation in MDA-231-MB cells when incubated at 4 °C (**Table S5**). Similar results were observed in Caco2 cells, except in the case of DMA_{tetra} which is inconclusive. These results suggest that the uptake of these guanidinium-rich copolymers occurs, regardless of the microstructure, *via* a combination of both membrane permeation and endocytic uptake. We then studied the internalisation of DMA_{stat} and $DMA_{diblock}$ by MDA-MB-231 cells *via* confocal microscopy to assess whether the monomer distribution had any effect on the cell uptake pathway (**Fig. 4**). At 37 °C, incubation for 2 h with either compound lead to the observation of punctate patterns of fluorescence, indicative of uptake *via* endocytosis. These were not colocalised with Lysotracker™

Red suggesting that the fluorescent compounds had not yet accumulated in the lysosomes after 2 h. However, following 16 h of incubation these puncta were found to mostly colocalise with the lysosomes, confirming that a significant proportion of the compounds were internalised *via* endocytosis. However, in the case of $DMA_{diblock}$, some of the fluorescence observed in cells incubated (following 2 or 16 h incubation at 37 °C) was found to be dispersed throughout the cytosol, which would indicate that a considerable amount of this compound was also taken up *via* a non-endocytotic pathway. This suggests that a greater proportion of the diblock copolymer crosses the membrane passively at 37 °C in comparison to the statistical copolymer equivalent. This is confirmed by the observation made when $DMA_{diblock}$ was incubated at 4 °C (**Fig. 4**), where a cytosolic distribution of $DMA_{diblock}$ may be easily discerned due to the absence of the highly fluorescent puncta.

According to HPLC chromatograms, the overall hydrophobicity of $DMA_{diblock}$ is higher than that of DMA_{stat}, which may be attributed to partial screening of the charges in the polycationic segment. While this difference may account for the apparent difference in cellular uptake behavior observed, differences in monomer distribution between DMA_{stat} and $DMA_{diblock}$ also need to be considered. Oda and co-workers previously explained differences in haemolytic activity between random- and block- amphiphilic copolymers by looking at differences in single-chain conformation.[33] Folding in aqueous solution resulted in a conformation of the diblock in which all the charges point outwards, thus limiting hydrophobic interactions between the diblock polymer and red blood cell membranes, as compared to the statistical equivalent. Goda and co-workers previously reported that amphipathic copolymers made of polar a poly(2-methacryloyloxyethyl phosphorylcholine) (pMPC) block and a hydrophobic poly(*n*-butyl methacrylate) (pBMA) block had the ability to directly translocate through the cell membrane.[47] In their system, the absence of the hydrophobic

block resulted in the disappearance of cytosolic fluorescence, suggesting that amphiphilicity is necessary for crossing the cell membrane. Hence, we argue that for the diblock copolymer the extent of electrostatic interaction between the soluble polymer chains and the membrane is less efficient due to steric crowding of the guanidinium moieties. However, once electrostatic binding is established, insertion into the membrane and direct translocation of the polymer is more effective by virtue of a substantial hydrophobic block. On the contrary, while the statistical polymer may be able to interact more with the membrane due to the more evenly distributed guanidinium groups, they lack hydrophobic domain needed to cross and escape complexation with the membrane, explaining why the statistical copolymer is mostly present in the vesicular pathway. This is in accordance with model studies by Sommer and co-workers which showed that amphiphilicity in statistical copolymers tends to increase surface effects but inhibit translocation across lipid bilayer membrane.[48] Increased interaction with the cell membrane would also account for the overall increased uptake of statistical polymers (DMA_{stat} and HEA_{stat}), as they possess higher affinity for the cell membrane and may thus be engulfed during endocytosis to a greater extent than their block copolymer equivalents.

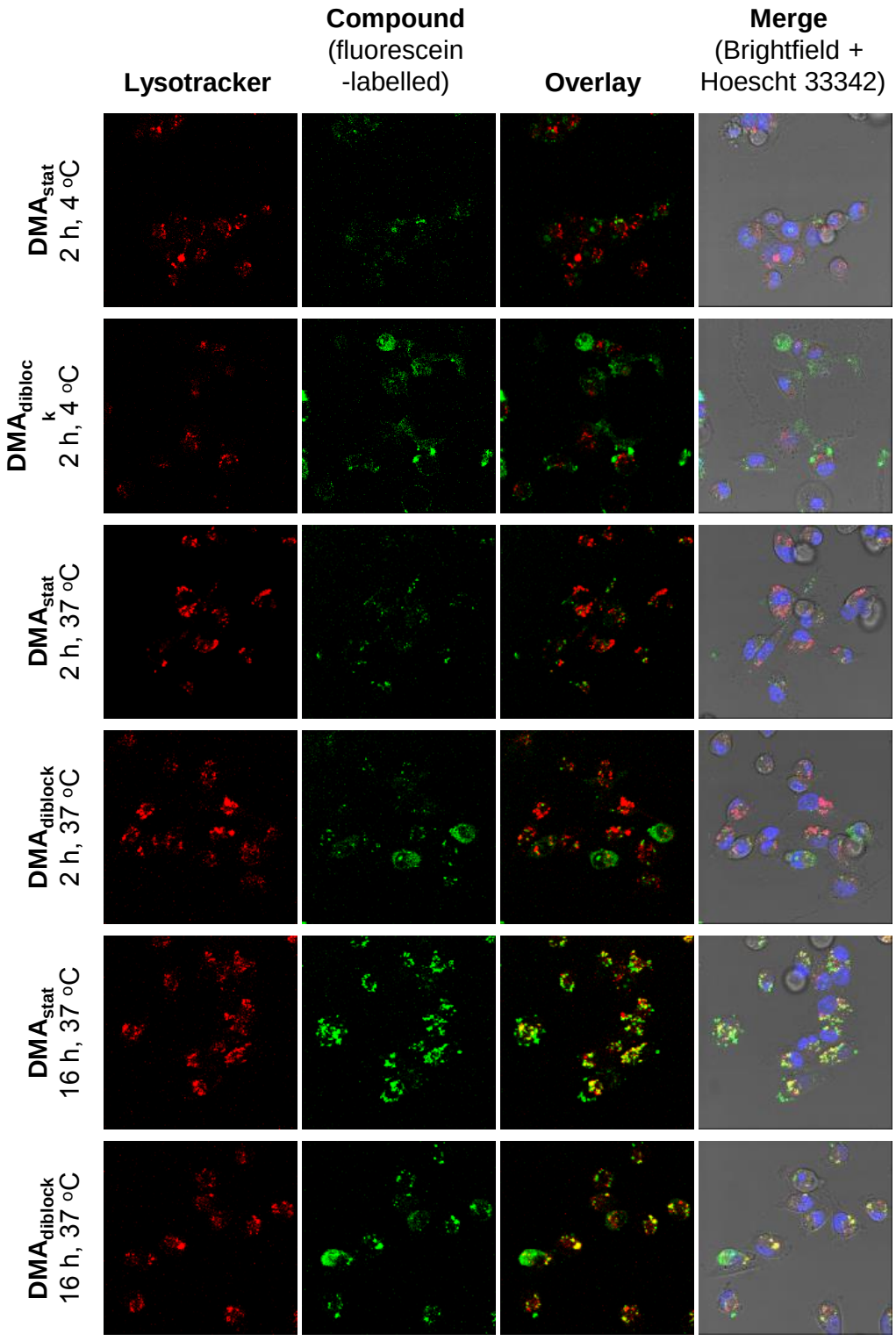

Figure 4. Confocal microscopic analysis of the intracellular location of DMA_{stat} and $DMA_{diblock}$ in live MDA-MB-231 cells following incubation at the indicated time and temperature Cells were

stained with Lysotracker™ Red and Hoechst 33342 to stain the lysosomes and nucleus, respectively. Co-localisation of the compounds with the lysosomes resulted in yellow spots in the overlay images.

4. CONCLUSION

We have prepared a range of guanidinium-rich linear polymers *via* RAFT polymerisation that are effective for intracellular uptake. Well-defined pGEA homopolymers ($Đ \approx 1.1$) were found to enter cells predominantly *via* passive membrane crossing, with enhanced overall uptake by cells in comparison to polyArginine peptide analogues commonly employed in modern drug delivery. Furthermore, an optimised RAFT polymerisation approach served as a powerful tool to introduce more hydrophobic monomers in the polymeric chains, and for the first time investigate the impact of monomer distribution on the cellular uptake of guanidinium-rich copolymers. Studying the cellular uptake of well-defined copolymers ($Đ < 1.2$) containing either DMA or HEA as comonomer, it was found that introducing hydrophobicity could lead to enhanced cellular uptake, with the statistically distributed copolymer system based on the more hydrophobic comonomer ($DMA_{stat} > HEA_{stat}$) seemingly experiencing the highest levels of internalisation. In contrast with the homopolymers, the copolymers studied were found to be internalised to a significant extent *via* both endocytotic and non-endocytotic means. We highlight that the overall hydrophobicity of these soluble polymer chains is not the sole parameter dictating the extent of cellular uptake, and that the monomer distribution has a profound influence on both the level of intracellular uptake and, interestingly, the mechanism by which the copolymer is internalised. While the statistical copolymers underwent intracellular uptake to a greater extent than their segmented counterparts,

confocal microscopy experiments would indicate that block copolymer microstructure is more partial towards passive membrane crossing. In all, this study represents a first step in understanding the fundamental influence of copolymer microstructure on cellular uptake. Using well-defined RAFT polymers as an alternative to polyArginine peptides provides easier-to-access materials and, through ready tuning of polymer composition and microstructure, could be used to modulate both the amount of material entering cells and their intracellular destination.

ASSOCIATED CONTENT

Supporting Information. The following files are available free of charge.

Compounds synthesis and characterisation, additional polymer characterisation (NMR, GPC, HPLC), cytotoxicity, additional cell uptake studies.

AUTHOR INFORMATION

Corresponding Author

* Prof. S. Perrier, Department of Chemistry, University of Warwick, Gibbet Hill Road, Coventry, CV4 7AL, UK.

E-mail: s.perrier@warwick.ac.uk.

Author Contributions

The manuscript was written through contributions of all authors. All authors have given approval to the final version of the manuscript. ⊥These authors contributed equally.

Funding Sources

Royal Society Wolfson Merit Award (WM130055; SP); Monash-Warwick Alliance (LM), European Research Council (TUSUPO 647106; SP, RP) and CSIRO (AK)

ACKNOWLEDGMENT

We thank the Royal Society Wolfson Merit Award (WM130055; SP), the Monash-Warwick Alliance (LM), European Research Council (TUSUPO 647106; SP, RP) and CSIRO (AK) for financial support. We are grateful for the Polymer Characterisation RTP for providing use of GPC/SEC.

REFERENCES

1. Bilensoy, E., Cationic nanoparticles for cancer therapy. *Expert Opinion on Drug Delivery* **2010,** 7, (7), 795-809.
2. Xu, F. J.; Yang, W. T., Polymer vectors via controlled/living radical polymerization for gene delivery. *Prog. Polym. Sci.* **2011,** 36, (9), 1099-1131.
3. Rinkenauer, A. C.; Schubert, S.; Traeger, A.; Schubert, U. S., The influence of polymer architecture on in vitro pDNA transfection. *Journal of Materials Chemistry B* **2015,** 3, (38), 7477-7493.
4. Gody, G.; Barbey, R.; Danial, M.; Perrier, S., Ultrafast RAFT polymerization: multiblock copolymers within minutes. *Polym. Chem.* **2015, 6**, (9), 1502-1511.
5. Gody, G.; Maschmeyer, T.; Zetterlund, P. B.; Perrier, S., Rapid and quantitative one-pot synthesis of sequence-controlled polymers by radical polymerization. **2013,** 4, 2505.
6. Gody, G.; Maschmeyer, T.; Zetterlund, P. B.; Perrier, S., Pushing the Limit of the RAFT Process: Multiblock Copolymers by One-Pot Rapid Multiple Chain Extensions at Full Monomer Conversion. *Macromolecules* **2014,** 47, (10), 3451-3460.
7. Gody, G.; Maschmeyer, T.; Zetterlund, P. B.; Perrier, S., Exploitation of the Degenerative Transfer Mechanism in RAFT Polymerization for Synthesis of Polymer of High Livingness at Full Monomer Conversion. *Macromolecules* **2014,** 47, (2), 639-649.
8. Kuroki, A.; Martinez-Botella, I.; Hornung, C. H.; Martin, L.; Williams, E. G. L.; Locock, K. E. S.; Hartlieb, M.; Perrier, S., Looped flow RAFT polymerization for multiblock copolymer synthesis. *Polym. Chem.* **2017,** 8, (21), 3249-3254.
9. Martin, L.; Gody, G.; Perrier, S., Preparation of complex multiblock copolymers via aqueous RAFT polymerization at room temperature. *Polym. Chem.* **2015,** 6, (27), 4875-4886.

10. Anastasaki, A.; Waldron, C.; Wilson, P.; Boyer, C.; Zetterlund, P. B.; Whittaker, M. R.; Haddleton, D., High molecular weight block copolymers by sequential monomer addition via Cu(0)-mediated living radical polymerization (SET-LRP): An optimized approach. *ACS Macro Lett.* **2013, 2**, (10), 896-900.
11. Anastasaki, A.; Nikolaou, V.; Pappas, G. S.; Zhang, Q.; Wan, C.; Wilson, P.; Davis, T. P.; Whittaker, M. R.; Haddleton, D. M., Photoinduced sequence-control via one pot living radical polymerization of acrylates. *Chem. Sci.* **2014, 5**, (**9**), 3536-3542.
12. Zhang, Q.; Collins, J.; Anastasaki, A.; Wallis, R.; Mitchell, D. A.; Becer, C. R.; Haddleton, D. M., Sequence-Controlled Multi-Block Glycopolymers to Inhibit DC-SIGN-gp120 Binding. *Angew. Chem., Int. Ed.* **2013,** 52, (16), 4435-4439.
13. Moraes, J.; Peltier, R.; Gody, G.; Blum, M.; Recalcati, S.; Klok, H.-A.; Perrier, S., Influence of Block versus Random Monomer Distribution on the Cellular Uptake of Hydrophilic Copolymers. *ACS Macro Lett.* **2016,** 5, (12), 1416-1420.
14. Silhol, M.; Tyagi, M.; Giacca, M.; Lebleu, B.; Vivès, E., Different mechanisms for cellular internalization of the HIV-1 Tat-derived cell penetrating peptide and recombinant proteins fused to Tat. *European Journal of Biochemistry* **2002,** 269, (2), 494-501.
15. Futaki, S.; Nakase, I., Cell-Surface Interactions on Arginine-Rich Cell-Penetrating Peptides Allow for Multiplex Modes of Internalization. *Accounts of Chemical Research* **2017,** 50, (10), 2449-2456.
16. Bechara, C.; Sagan, S., Cell-penetrating peptides: 20 years later, where do we stand? *FEBS Lett.* **2013,** 587, (12), 1693-1702.
17. Zorko, M.; Langel, Ü., Cell-penetrating peptides: mechanism and kinetics of cargo delivery. *Advanced Drug Delivery Reviews* **2005,** 57, (4), 529-545.
18. Sakai, N.; Futaki, S.; Matile, S., Anion hopping of (and on) functional oligoarginines: from chloroform to cells. *Soft Matter* **2006,** 2, (8), 636-641.
19. Gasparini, G.; Bang, E. K.; Montenegro, J.; Matile, S., Cellular uptake: lessons from supramolecular organic chemistry. *Chem. Commun.* **2015,** 51, (52), 10389-10402.
20. Wender, P. A.; Mitchell, D. J.; Pattabiraman, K.; Pelkey, E. T.; Steinman, L.; Rothbard, J. B., The design, synthesis, and evaluation of molecules that enable or enhance cellular uptake: Peptoid molecular transporters. *Proceedings of the National Academy of Sciences* **2000,** 97, (24), 13003-13008.
21. Wender, P. A.; Rothbard, J. B.; Jessop, T. C.; Kreider, E. L.; Wylie, B. L., Oligocarbamate Molecular Transporters: Design, Synthesis, and Biological Evaluation of a New Class of Transporters for Drug Delivery. *J. Am. Chem. Soc.* **2002,** 124, (45), 13382-13383.
22. Cooley, C. B.; Trantow, B. M.; Nederberg, F.; Kiesewetter, M. K.; Hedrick, J. L.; Waymouth, R. M.; Wender, P. A., Oligocarbonate Molecular Transporters: Oligomerization-Based Syntheses and Cell-Penetrating Studies. *J. Am. Chem. Soc.* **2009,** 131, (45), 16401-16403.
23. McKinlay, C. J.; Waymouth, R. M.; Wender, P. A., Cell-Penetrating, Guanidinium-Rich Oligophosphoesters: Effective and Versatile Molecular Transporters for Drug and Probe Delivery. *J. Am. Chem. Soc.* **2016,** 138, (10), 3510-3517.
24. Exley, S. E.; Paslay, L. C.; Sahukhal, G. S.; Abel, B. A.; Brown, T. D.; McCormick, C. L.; Heinhorst, S.; Koul, V.; Choudhary, V.; Elasri, M. O.; Morgan, S. E., Antimicrobial Peptide Mimicking Primary Amine and Guanidine Containing Methacrylamide Copolymers Prepared by Raft Polymerization. *Biomacromolecules* **2015,** 16, (12), 3845-3852.

25. Treat, N. J.; Smith, D.; Teng, C.; Flores, J. D.; Abel, B. A.; York, A. W.; Huang, F.; McCormick, C. L., Guanidine-Containing Methacrylamide (Co)polymers via aRAFT: Toward a Cell-Penetrating Peptide Mimic. *ACS Macro Lett.* **2012,** 1, (1), 100-104.
26. Parsons, K. H.; Holley, A. C.; Munn, G. A.; Flynt, A. S.; McCormick, C. L., Block ionomer complexes consisting of siRNA and aRAFT-synthesized hydrophilic-block-cationic copolymers II: the influence of cationic block charge density on gene suppression. *Polym. Chem.* **2016,** 7, (39), 6044-6054.
27. Koschek, K.; Dathe, M.; Rademann, J., Effects of Charge and Charge Distribution on the Cellular Uptake of Multivalent Arginine-Containing Peptide-Polymer Conjugates. *Chembiochem* **2013,** 14, (15), 1982-1990.
28. Marie, E.; Sagan, S.; Cribier, S.; Tribet, C., Amphiphilic Macromolecules on Cell Membranes: From Protective Layers to Controlled Permeabilization. *Journal of Membrane Biology* **2014,** 247, (9-10), 861-881.
29. Sarapas, J. M.; Backlund, C. M.; deRonde, B. M.; Minter, L. M.; Tew, G. N., ROMP- and RAFT-Based Guanidinium-Containing Polymers as Scaffolds for Protein Mimic Synthesis. *Chemistry – A European Journal* **2017,** 23, (28), 6858-6863.
30. deRonde, B. M.; Tew, G. N., Development of protein mimics for intracellular delivery. *Peptide Science* **2015,** 104, (4), 265-280.
31. Hennig, A.; Gabriel, G. J.; Tew, G. N.; Matile, S., Stimuli-Responsive Polyguanidino-Oxanorbornene Membrane Transporters as Multicomponent Sensors in Complex Matrices. *J. Am. Chem. Soc.* **2008,** 130, (31), 10338-10344.
32. Geihe, E. I.; Cooley, C. B.; Simon, J. R.; Kiesewetter, M. K.; Edward, J. A.; Hickerson, R. P.; Kaspar, R. L.; Hedrick, J. L.; Waymouth, R. M.; Wender, P. A., Designed guanidinium-rich amphipathic oligocarbonate molecular transporters complex, deliver and release siRNA in cells. *Proceedings of the National Academy of Sciences* **2012,** 109, (33), 13171-13176.
33. Oda, Y.; Kanaoka, S.; Sato, T.; Aoshima, S.; Kuroda, K., Block versus Random Amphiphilic Copolymers as Antibacterial Agents. *Biomacromolecules* **2011,** 12, (10), 3581-3591.
34. Sgolastra, F.; Minter, L. M.; Osborne, B. A.; Tew, G. N., Importance of Sequence Specific Hydrophobicity in Synthetic Protein Transduction Domain Mimics. *Biomacromolecules* **2014,** 15, (3), 812-820.
35. Backlund, C. M.; Sgolastra, F.; Otter, R.; Minter, L. M.; Takeuchi, T.; Futaki, S.; Tew, G. N., Increased hydrophobic block length of PTDMs promotes protein internalization. *Polym. Chem.* **2016,** 7, (48), 7514-7521.
36. Sgolastra, F.; Backlund, C. M.; Ilker Ozay, E.; deRonde, B. M.; Minter, L. M.; Tew, G. N., Sequence segregation improves non-covalent protein delivery. *J Control Release* **2017,** 254, 131-136.
37. Ferguson, C. J.; Hughes, R. J.; Nguyen, D.; Pham, B. T. T.; Gilbert, R. G.; Serelis, A. K.; Such, C. H.; Hawkett, B. S., Ab Initio Emulsion Polymerization by RAFT-Controlled Self-Assembly. *Macromolecules* **2005, 38**, (6), 2191-2204.
38. Scudiero, D. A.; Shoemaker, R. H.; Paull, K. D.; Monks, A.; Tierney, S.; Nofziger, T. H.; Currens, M. J.; Seniff, D.; Boyd, M. R., Evaluation of a Soluble Tetrazolium/Formazan Assay for Cell Growth and Drug Sensitivity in Culture Using Human and Other Tumor Cell Lines. *Cancer Research* **1988,** 48, (17), 4827-4833.
39. Porel, M.; Thornlow, D. N.; Phan, N. N.; Alabi, C. A., Sequence-defined bioactive macrocycles via an acid-catalysed cascade reaction. *Nat Chem* **2016,** 8, (6), 590-596.

40. Alhakamy, N. A.; Berkland, C. J., Polyarginine Molecular Weight Determines Transfection Efficiency of Calcium Condensed Complexes. *Molecular Pharmaceutics* **2013,** 10, (5), 1940-1948.
41. Mitchell, D. J.; Kim, D. T.; Steinman, L.; Fathman, C. G.; Rothbard, J. B., Polyarginine enters cells more efficiently than other polycationic homopolymers. *Journal of Peptide Research* **2000,** 56, (5), 318-325.
42. Futaki, S.; Suzuki, T.; Ohashi, W.; Yagami, T.; Tanaka, S.; Ueda, K.; Sugiura, Y., Arginine-rich peptides - An abundant source of membrane-permeable peptides having potential as carriers for intracellular protein delivery. *Journal of Biological Chemistry* **2001,** 276, (8), 5836-5840.
43. Fretz, M. M.; Penning, N. A.; Al-Taei, S.; Futaki, S.; Takeuchi, T.; Nakase, I.; Storm, G.; Jones, A. T., Temperature-, concentration- and cholesterol-dependent translocation of L- and D-octa-arginine across the plasma and nuclear membrane of CD34(+) leukaemia cells. *Biochemical Journal* **2007,** 403, 335-342.
44. Liu, Z. H.; Zhang, Z. Y.; Zhou, C. R.; Jiao, Y. P., Hydrophobic modifications of cationic polymers for gene delivery. *Prog. Polym. Sci.* **2010,** 35, (9), 1144-1162.
45. Barz, M.; Luxenhofer, R.; Zentel, R.; Kabanov, A. V., The uptake of N-(2-hydroxypropyl)-methacrylamide based homo, random and block copolymers by human multi-drug resistant breast adenocarcinoma cells. *Biomaterials* **2009,** 30, (29), 5682-5690.
46. Rothbard, J. B.; Kreider, E.; VanDeusen, C. L.; Wright, L.; Wylie, B. L.; Wender, P. A., Arginine-Rich Molecular Transporters for Drug Delivery: Role of Backbone Spacing in Cellular Uptake. *Journal of Medicinal Chemistry* **2002,** 45, (17), 3612-3618.
47. Goda, T.; Goto, Y.; Ishihara, K., Cell-penetrating macromolecules: Direct penetration of amphipathic phospholipid polymers across plasma membrane of living cells. *Biomaterials* **2010,** 31, (8), 2380-2387.
48. Werner, M.; Sommer, J. U., Translocation and Induced Permeability of Random Amphiphilic Copolymers Interacting with Lipid Bilayer Membranes. *Biomacromolecules* **2015,** 16, (1), 125-135.

1 TOC